

HOROLOGICAL SCIENCE NEWSLETTER NAWCC CHAPTER #161 www.hsn161.com

Issue 2023-1 February 2023

Bob Holmström, Editor & Publisher, 2934 NW 53rd Drive, Portland, OR 97210
Phone: 503-292-3685, holmstro@gmail.com
John Haine, Assistant Editor, john.haine@haine-online.net
Tom Van Baak, Assistant Editor, tvb@LeapSecond.com
David Spong, Secretary & Treasurer, 31120 Marne Drive, Ranch Palos Verdes,
CA 90275 Phone: 310 541-4150, edavid.spong@verizon.net

<u>Page</u>	<u>Contents</u>
2 - 22	From the medieval Verge & Foliot clock to the Harrison H4 timekeeper - joint physical aspects of the improvement in accuracy by Dieter Roess
23 - 26	Experimental Snippet: Eddy Current Fly by Mike Everman
27 - 30	The mechanics of a compound pendulum comprising two point masses by Martin Rice

Announcing the Horological Science Newsletter forum

Years ago it was common for HSN readers to comment on articles by publishing short letters or essays which would appear in the next issue. In many cases this was the only way to contact the author. The written dialog was a valuable asset to the HSN community. However, this practice has fallen out of favor now that everyone communicates electronically and no one wants to wait months to post commentary or half a year to receive a reply. So, we have created a HSN forum to facilitate direct reader and author communication:

<https://groups.io/g/Horological-Science-Newsletter>

The groups.io domain is well-known for hosting web forum / mailing lists. Signing up is simple and free. Articles will still, of course, be published in HSN, but this forum will allow rapid follow-up communication among readers and authors. The forum is open to anyone although we expect it will consist mostly of HSN members. The topics of discussion should revolve around HSN articles, either recently published or works in progress.

A decision is being made about online access to the full HSN archive. We hope to announce that by the next issue.

-- the editors

The deadline for material for the next issue is ????. Material is urgently needed – there is nothing in the queue. An issue will be emailed when sufficient material is available. Bob Holmström

Above: Drawing from Apians cosmographic Liber of 1533, showing how a nocturnal is used to tell the time at night from the Great Bear.

From the medieval Verge & Foliot clock to the Harrison H4 timekeeper - joint physical aspects of the improvement in accuracy

Dieter Roess

Introduction

From about 1300 until around 1700 the simple and sturdy *Verge & Foliot* turret clock (V&F)¹ was the common public timekeeper, announcing time by one or two hands at a dial, and clocks triggered at hour or quarter hour intervals. In view of its broad application, its accuracy seems to have fulfilled the then public needs.

Accuracy useful for astronomical observation had been achieved in small precision clocks with the *Cross Beat* escapement, invented 1584 by Jost Bürgi [1]. It uses two one-pallet verges coupled to two foliots. The complicated construction prevented its use in public clocks.

After the discovery of the oscillatory characteristics of a pendulum, a *Verge & Pendulum* (V&P) clock was demonstrated by Ch. Huygens in about 1656 [2], replacing the foliot by a pendulum, and achieving a substantial gain in accuracy. As the change of V&F clocks into V&P ones was easy, public clocks were transformed within a few decades (thus, it is doubtful if current V&F turret clocks survived in original state).

The next improvement was the introduction of the anchor instead of the verge at about 1660², combined with a pendulum or spring, which became the basis of most future improvements³.

Surprisingly, in 1759 John Harrison [3] returned to the verge (and spiral) escapement in his famous H4⁴, which was an outstanding landmark in accuracy, for the first time allowing a simple calculation of geographical longitudinal distance and revolutionizing the position-finding of ships on sea.

There are no historical reports about the accuracy of the medieval Verge and Foliot clocks. A daily deviation of 15 minutes is quoted in many publications, with no reported source of such a value. With newly constructed clocks the author and others recorded daily fluctuations of about 1 minute over longer periods, with unexplained drifts and sudden jumps in between; comparable results were obtained with a turret clock dated 1478 reconstructed by the author⁵.

For the *Cross Beat* clock of Jost Bürgi, exhibited at the Landesmuseum Kassel⁶, an accuracy of ± 30 s/d is quoted [1]. The verge and Pendulum clock of Ch. Huygens is reported to have achieved an accuracy of 10 s/d [4].

Anchor escapements achieve accuracies below 1 s/d if secondary influences are compensated, in their most refined versions below 1/100 s/day.

¹ picture of the famous Dover clock <https://mostre.museogalileo.it/motoperpetuo/en/after-leonardo/between-uncertainty-and-fraud/mechanism-for-a-bell-tower-clock-with-verge-escapement-and-foliot.html>

² Robert Hook and William Clement both claimed to be its inventors.

³ animated simulation see <https://redfernanimation.com/the-anchor-escapement/>

⁴ a very detailed animation: <https://redfernanimation.com/the-harrison-timekeepers/>

⁵ Roess "Wie genau gingen die großen Foliot-Turmuhren (Spindel mit Waag) des Mittelalters" p. 38 CHRONOMETROPHILIA No. 81 2017

⁶ <https://datenbank.museum-kassel.de/46943/0/0/0/4/0/objekt.html>

The Harrison H4 is reported to have achieved an accuracy (*being slow*) of 5s in 81 days, on its first travel at sea [5].

Friction, Randomness and Accuracy

There is a rich literature concerning the function of early clocks. The 1953 paper by von Bertele [6], and the 2004 paper by Kees Grimbergen [7] are of special historic interest. The authors analyze and compare the V&F and the V&P and escapements. In these early treatments, as in those of most successors, the crucial role of the drive weight as part of the V&F oscillator is neglected, denying the V&F escapement the characteristics of a “true” oscillator as consequence, and overestimating the contribution of the *fall*⁷- impact as drive to the pallets, compared to the much higher one of continuous torque. Very early, the high friction in the verge escapements was recognized, without analyzing its origin and its physical effect on accuracy. Taking into consideration these details, an understanding of all kinds of escapements under a general view can be achieved, and that is the goal of this paper.

All escapements mentioned are damped oscillators with synchronous feedback from some mechanical energy source (a descending weight in the gravitational field or relaxing compression in a spring) to compensate the energy loss caused by friction in the escapement, the size and effect of which is highly different for diverse geometrical configurations.

Independent of its value, constant friction should not lead to a deviation of oscillation periods, and of clock time as the sum of clock periods.

Periodic changes in oscillator period, as caused by changing drive weight due to the varying active length of the rope or to a decrease of drive spring power, will lead to a periodic variation of period and clock time, that should average out in times longer than the periods of change. At the range of days, this is true also for interruption of the clock operation during winding up of weight or spring.

In contrast, unforeseeable fluctuations of clock parameters as drive or friction, which can be classified as *random* either or both in time and size will lead to random fluctuations of period, the sum of which as *clock time* will not average out at any time scale. Rather, clock time will perform a “random walk” in time, that is unforeseeable in detail for the individual run. The deviation from standard time then will fluctuate within limits that increase with time.

A common example of random walk is throwing a coin and betting on “head” or “tail”. In a regular game the changes should be 1:1. Randomness of the throws will let head or tail fluctuate at random, and the money accumulating at one player will follow a *random walk*. At the extreme, it is limited to the sum or loss of all bets within a “lucky strike”, but it will fluctuate within much lower limits at a “normal” one of many games.

In the present analysis, the physical mechanism of fluctuations in friction is important. Hence, the phenomenon of random walk is visualized in some detail.

⁷ *fall*: the free impact between one pair of tooth and pallet at release of the other one.

A	B	C
time	random nr	sum
1	=2*(ZUFALLSZAHL()-0.5)	=C9+B10
2	=2*(ZUFALLSZAHL()-0.5)	=C10+B11
3	=2*(ZUFALLSZAHL()-0.5)	=C11+B12
4	=2*(ZUFALLSZAHL()-0.5)	=C12+B13
5	=2*(ZUFALLSZAHL()-0.5)	=C13+B14
6	=2*(ZUFALLSZAHL()-0.5)	=C14+B15
7	=2*(ZUFALLSZAHL()-0.5)	=C15+B16
8	=2*(ZUFALLSZAHL()-0.5)	=C16+B17
9	=2*(ZUFALLSZAHL()-0.5)	=C17+B18

The phenomenon is conveniently studied using *Excel*, with its function for producing random numbers⁸.

For a time-series (column A) the function in column B1 creates a random number between -1 and +1. Copying the first cell to the column creates a series of different random numbers. When any cell in the table is activated by *double click* and *Enter*, a new series is created.

The formula in column C is the sum of samples B and corresponds to the random walk of accumulated time.

In figure 1 two series (red and blue) of random samples are superimposed in the left graph, corresponding to fluctuations of the escapement period within a range of ± 1 . One may be misled to see some periodicities or singular disturbances, but there is just randomness. No systematic difference can be recognized between the two different sample runs.

Figure 2 shows the fluctuation sums of 10 independent runs. They correspond to the difference of individual clock time runs against their average (standard) time. While the patterns may differ widely for individual runs, the time dependence of deviation from standard in most runs will stray within the red, dotted parabola, which characterizes the square root of the number of samples with fluctuation between -1 and +1. This behavior has consequences as to the judgement of accuracy in clocks. One

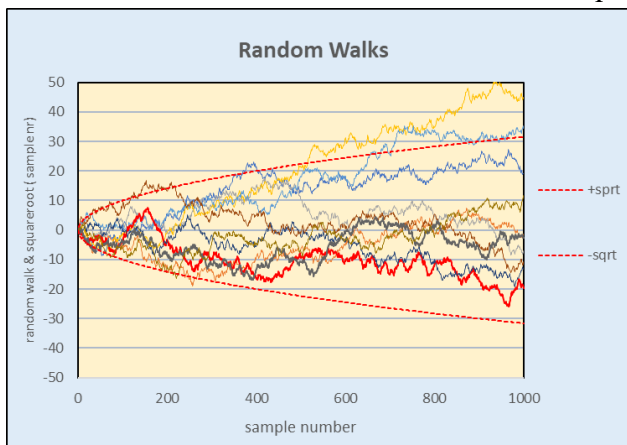


Figure 1



Figure 2

cannot base it upon the performance at a single run, as it may by chance have a close to zero random walk. One should observe a sufficient number of independent runs and then define accuracy as a proper average of them. Also, one cannot take the deviation at a certain time and then define accuracy as this deviation divided by the time interval involved: a random walk with wild fluctuations could just have crossed the zero line at that time⁹.

The random pattern also characterizes the difficulty of tuning a clock operating close to its limits of accuracy, to some standard time. Deviation at a specific time is no good measure, as it may be far from the long-time average - “tuning” then may lead to a still stronger mistuning. A better measure is to use the average over a sufficiently long time; even this is no guarantee - tuning remains a trial-and-error process as one approaches the limit of fluctuation.

⁸ *Zufallszahl()* is used in the German version. It will be *random()* in the English one.

⁹ Insofar, the report on the Harrison H4 being slow by 5s in 81 days does *not* say that its daily variation was 5/81 sec.

Friction is a process at atomic scale and needs a simplified model to arrive at some applicable rules. It is generally assumed that the atomic process is close to proportional to

- the relative speed between two contacting parts.
- the pressure between contacting parts.
- the amount of friction energy applied in a certain time (clock period).

Relative speed of contact between tooth and pallet is changing during the period. It is zero at the oscillation maxima and also when pallet and tooth flank are parallel (at zero pallet arc for teeth that are not undercut). For the further discussion we will concentrate on friction energy and friction pressure as the main factors for fluctuations in period.

Friction energy

In a clock escapement, the friction energy dissipated during one period is equal to the energy loss of the feedback energy source (the descending drive mass, the spring unwinding) within that time.

In a real clock, part of the friction energy is absorbed in bearings and contacts of the train: F_{train} . With careful construction and lubrication, by far most of the friction energy is absorbed in the central part of the escapement, the contact between tooth and pallet: F_P . A small part of escapement friction is absorbed by air resistance to the fastmoving parts of the escapement – foliot, pendulum or balance, and is finally dissipated as heat to the air F_{air} .

$$Energy\ loss\ of\ drive = F_{train} + F_P + F_{air} . ,$$

In general, friction in air is small compared to that in gear and pallet contact and must be considered only in high precision pendulum clocks. Train friction can be reduced by careful construction and lubrication yet is not negligible in turret clocks; there, it acts like as a reduction of the drive available at the pallet contact, introducing some stochastic element of its own.

Pallet contact friction F_P is the largest consumer of drive energy in the early clocks, and its analysis is the interesting issue in this paper.

V&F escapement.

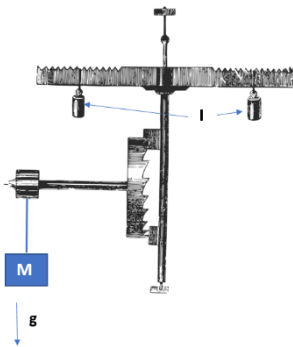


Figure 3

In the V&F (figure 3)¹⁰, the oscillator consists of interaction between the inertia I of the foliot and gravitational attraction g of the drive weight mass M , with Mg assumed to act directly upon the pallet¹¹. When the foliot accelerates with increasing rotational energy, the drive weight descends, losing gravitational energy; when the foliot decelerates, the drive weight rises, gaining gravitational energy [8].

This combination has no natural equilibrium position. To change direction, the maximum rotational energy of the foliot must be completely dissipated by friction and the same energy applied as feedback to achieve maximum rotational energy in the opposite direction of rotation. The energy absorbed

¹⁰Basic picture in https://en.wikipedia.org/wiki/Verge_escapement

¹¹ The torque exercised at the pallet is related to the torque of the weight at the bottom wheel barrel by the gear factor between bottom wheel and crown wheel (typically 10), and the radius relation of barrel and crown wheel (typically 1/2), resulting in a factor of typically 20.

in one period for direction change corresponds to twice the maximum rotational energy of the foliot and is absorbed at the pallet/tooth contact.

With I the inertia of the foliot, its rotational energy is $J = I \frac{\dot{\varphi}^2}{2}$; $I = Mr^2$, $\dot{\varphi}$ being the angular velocity (time derivative) of the foliot arc φ , M the mass of the foliot (mostly concentrated at its runners, the tuning weights at the foliot bar), and r the distance of Mass M from the foliot axis.

While the dynamics (time dependence) of the angular velocity is quite complicated and needs two different nonlinear differential equations for complete description [9], one can describe the dependence of the oscillation period on the fixed escapement parameters at typical oscillation amplitudes and pallet length L approximately by the formula¹².

$$T = 2\pi \sqrt{\frac{I}{gML}} \rightarrow M \approx \frac{I}{gL} \left(\frac{2\pi}{T} \right)^2$$

The relation means that a certain oscillation period needs a well-defined relation of drive mass to foliot inertia. With typical data of a V&F turret clock: $T = 8s$; $L = 2cm$; $I = 450000gcm^2$ (at $M = 500g$; $r = 30cm$), the drive active at the pallet necessary to achieve rotation reversal corresponds to $M \approx 70g$. With a gear ratio of 10 between hour wheel and escape wheel, and a relation of wheel radii of 2, drive weight mass at the hour wheel is about 1400g.

In one period, the drive weight descends by 1 tooth distance of the escape wheel divided by the gear radii, to achieve the twofold reversal of foliot rotation and this loss in gravitational energy must be absorbed by friction at the tooth pallet contact.

In between, the drive weight oscillates up and down, storing gravitational energy; yet the stored energy is less than 50% of the “dissipated one” at typical oscillation amplitudes.

Verge and Pendulum in comparison to Verge and Foliot

In the V&P (figure 4)¹³, the oscillator consists in the interaction between the rotational energy of the pendulum and the gravitational energy of the pendulum itself. Both are proportional to the mass of the pendulum and its distribution along its length¹⁴. When the pendulum accelerates with increasing rotational energy, it descends - losing gravitational energy; when the pendulum decelerates, it rises -

¹² The formula is quite similar to the well-known one of the pendulum at very low amplitude. With the pendulum $I=ML^2$, leading to $T = 2\pi \sqrt{\frac{L}{g}}$. The difference in period mainly results from L being the pendulum length of typically 60 to 100 cm, or L being the pallet length of typically 2 to 3cm.

¹² <https://redfernanimation.com/>

¹² It is commonly assumed that the pendulum mass is concentrated in a point-like bob at distance L from the center of rotation.

¹² <https://redfernanimation.com/>

¹² It is commonly assumed that the pendulum mass is concentrated in a point-like bob at distance L from the center of rotation.

¹³ <https://redfernanimation.com/>

¹⁴ It is commonly assumed that the pendulum mass is concentrated in a point-like bob at distance L from the center of rotation.

gaining gravitational energy. This is analogous to the energy exchange between foliot and drive weight V&F.



Figure 4

This combination has a natural equilibrium position at minimum gravitational and maximum rotational energy (the lowest position of the pendulum center of gravity). Change in direction is automatically achieved by the unidirectionality of the gravitational field and thus sign of rotation change is achieved without energy consumption. To sustain constant amplitude, feedback must just restore the energy loss of the pendulum in air, in the bearings and the pallet friction for those two contributions.

Thus, the total energy absorbed in one period at the pallet is much smaller in the V&P than in the V&F. The basic physical difference is the utilization of the unidirectionality of the gravitational field in the pendulum for inversion of the sense of rotation, while in the V&T this is achieved by friction.

The same argument holds for a verge watch with balance and spring. Here the symmetry of the elastic deformation of the spring creates a minimum potential energy point, that causes an automatic inversion of the sense of rotation of the balance, without the need of inversion energy.

In the differential equation of oscillators, friction energy is characterized by a friction coefficient R . It can be visualized and determined easily by measuring the exponential increase of amplitude from zero with drive weight applied, or by decay of an oscillation when cutting off drive weight (the latter procedure is not possible in the V&F, as the drive weight is both part of the oscillator and feedback source). The calculated left and middle graphs in figure 6 show both patterns for an equal, high friction coefficient.

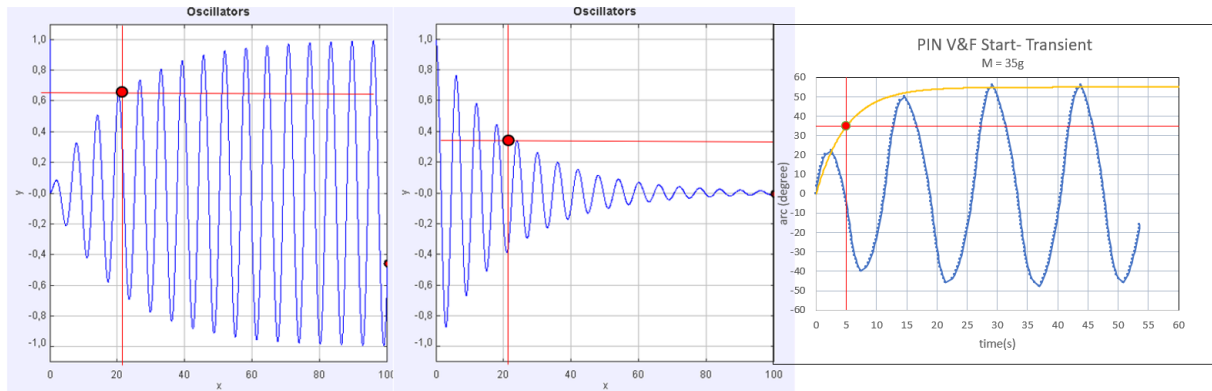


Figure 5

The coefficient itself can be obtained by counting the number of oscillations Z till $(1-1/e)$ of the final amplitude is achieved at increasing amplitude (left graph), or $1/e$ at decay (center graph). These markers are drawn in the graphs as horizontal red lines. In both graphs the number of full periods is $Z = 3.9$, which corresponds to a friction coefficient $R = 1/eZ \approx 0.1$

The right graph shows a measured transient pattern of a new V&F clock. Here $Z = 0.50$ periods and $R = 1/eZ = 0.7$

With an old Verge & Pendulum turret clock, about 7 periods were observed till decay of the pendulum amplitude to $1/e$ ¹⁵. This corresponds to $R = 0.05$.

Thus, friction energy loss in the V&P escapement is about 20 times smaller than in an otherwise comparable V&F, as consequence of abolition of the inversion energy friction.

Friction Pressure in Verge escapements

Stochastic fluctuations in amplitude or period are assumed to largely be a consequence of friction, and friction caused material defects at pallet and tooth. Such an effect will be proportional to pressure, the quotient of friction energy divided by the area of contact. Therefore, it is important to analyze the size of the contact area.

Observing a real verge escapement, one may get the visual impression that in acceleration the full width of the tooth drives the plane pallet, while in deceleration the pallet rim contacts the tooth front plane¹⁶. Thus, the contact always seems to be along a line.

Yet, this impression is misleading and due to the small arcs involved. In reality the contact is in a single point [9]. This fact can be argued quite generally:

- Any point at the rim of the tooth or at its flank lies on a cylinder around the escape wheel axis
- Any point at the pallet plane lies on a cylinder around the axis of the verge, which is perpendicular to the one of the escape wheel.
- Any point of the escape wheel tooth rim lies in a plane that is perpendicular to the escape wheel axis.

These are three 3D-surfaces, which for geometrical reasons necessarily cut each other in a single point. Only when surfaces are *degenerate* (have common line or surface elements in 3D), they will cut along a 3D-curve or a plane (at zero pallet arc when pallet plane and tooth rim are parallel)

The consequence of this is decisive. While it is difficult to define what a “line contact” or “point contact” means at atomic scale, it is obvious that friction pressure is by orders of magnitude larger in a point than in a line contact at equal friction energy.

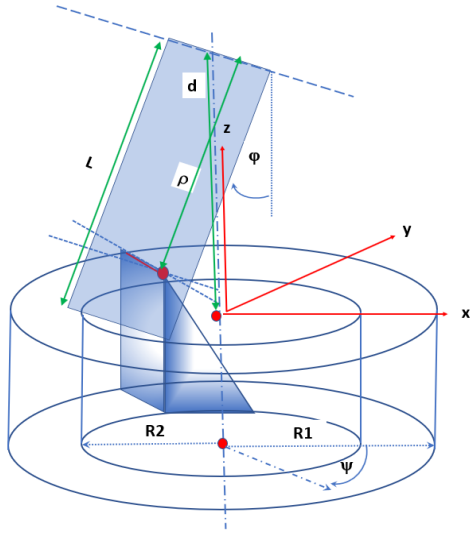
In a real physical contact, there will always a cushion of abrasion material and semifluid lubrication material between both solid materials, that distributes point or line pressure to some microscopic, but finite area.

As this is a decisive postulate for the following discussion, it appears worthwhile to derive an analytical solution of the contact point path during a full oscillation.

¹⁵ For this measurement the intermediary crown wheel should be detached, as it may have high friction loss that is not part of the oscillator loss, but of the clock gear.

¹⁶ This is true for teeth without undercut. At high undercut the contact may be restricted to the tooth rim.

In figure 6 the geometric situation is illustrated.



The edge of the tooth lies in the x - y plane. It moves in a circle around the z -axis of the crown wheel.

The width of the tooth is characterized by two radii $R1$ and $R2$ in the x - y plane. The tooth edge is at angle ψ from the x -axis.

The axis of the verge is perpendicular to the one of the crown wheel, oriented in the x -direction, and at distance d from the tooth plane. The pallet with length L moves in a circle around the verge axis.

The pallet touches the inner tooth edge a distance ρ from the verge axis. It is at angle ϕ from the z -axis.

Figure 6

Pointwise Contact between 3 Surfaces in Space xyz

Definitions :

- a.) Crown wheel axis: $x = 0; y = 0; z$
- b.) Pallet axis: $x, y = 0, z = d$
- c.) Distance on pallet from axis : ρ
- d.) Pallet arc in yz -plane: ϕ
- e.) Pallet length: L
- f.) Distance of tooth from verge axis: R
- g.) Tooth width: $R_2 \leq R \leq R_1$
- h.) Tooth arc in xy -plane: ψ

With these definition of the axis in space, the arcs involved and the distances from the axis, the three 3D- surfaces are::

Three 3D - surfaces

- 1.) $\phi > 0$ Tooth rim $x_1, y_1; z_1 = 0;$
 $\phi < 0$ Tooth inner flank $x_1 = R_2 \cos \psi, y_1 = R_2 \sin \psi; z_1 = d - L \cos \phi$
- 2.) Tooth cylinder $\sqrt{x_2^2 + y_2^2} = R^2; x_2 = R \cos \psi; y_2 = R \sin \psi; z_2;$
- 3.) Pallet cylinder $\sqrt{x_3^2 + y_3^2} = \rho^2; x_3; y_3 = \rho \sin \phi; z_3 = d - \rho \cos \phi$

As the tooth is impenetrable, the tooth contact plane is different for positive and negative pallet arcs.

The common points of two of these surfaces result as lying on 3D-lines, 1+2 with $\phi > 0$ resulting in the flat circle of the tooth tips, 2+3 in the 3D cutting line of the verge and the escape wheel cylinders, with variable parameters R and ρ .

The common points of all three surfaces result as a single point.

Common Points of three 3D - Surfaces $\varphi > 0$

1.) + 2.) + 3.) \rightarrow

$$x_1 = x_2 = x_3; y_1 = y_2 = y_3; z_1 = z_2 = z_3$$

$$z \rightarrow \rho = \frac{d}{\cos \varphi}; y \rightarrow y = R \sin \psi = \frac{\rho}{R} \sin \varphi \Rightarrow \sin \psi = \frac{d}{R} \operatorname{tg} \varphi$$

$$x = \sqrt{R^2 - d^2 \operatorname{tg}^2 \varphi}; y = d \operatorname{tg} \varphi; z = 0$$

\Rightarrow Unique point with 1 variable φ for given parameters R, d

Common points of three 3D surfaces $\varphi < 0$

1.) + 2.) + 3.) \rightarrow

$$x: x = R \cos \psi = R_2 \cos \psi; y: y = R \sin \psi = \rho \sin \varphi = R_2 \sin \psi;$$

$$z = d - \rho \cos \varphi = d - L \cos \varphi$$

$$\Rightarrow R = R_2; \rho = L; \sin \psi = \frac{L}{R_2} \sin \varphi$$

$$x = \sqrt{R_2^2 - L^2 \sin^2 \varphi}; y = L \sin \varphi; z = d - L \cos \varphi$$

For given parameters d and φ the three surfaces have just one common point.

The limits of parameters are

Limits

1.) solid pallet plane & $R_1 > R_2 \Rightarrow \varphi \geq 0 \rightarrow R = R_1; \varphi \leq 0 \rightarrow R = R_2$

2.) escape of leading tooth edge $\Rightarrow \rho = L \rightarrow \cos \varphi = \frac{d}{L};$

3.) escape from the tooth $\Rightarrow \operatorname{real} \sqrt{R_1^2 - (d)^2 \operatorname{tg}^2 \varphi} \rightarrow \operatorname{tg} \varphi = \frac{R_1}{d}$

4.) release of opposite pallet $\rightarrow \operatorname{tg} \varphi = \frac{R_2}{d}$ (at pallet angle of $\frac{\pi}{2} \equiv 90$ degrees)

5.) impact $\rightarrow \varphi = \frac{\pi}{2} - \arctan\left(\frac{R_2}{d}\right)$

- 1) With a solid, impenetrable pallet, and the far tooth limit being more distant from the escape wheel axis than the close one, the contact point is at the outer limit for positive arcs and at its inner one for negative arcs.
- 2) The distance from the verge axis cannot be larger than the pallet length.
- 3) The x -position must be real.

Figure 7 shows the calculated distance of the contact point at the pallet plane from the verge axis as function of the verge arc. The pattern starts at the impact of the tooth at the pallet (black vertical line), close to the minimum distance d from the verge axis.

For better visual demonstration, the tooth thickness ($R1-R2$) and the pallet parameters d and L (in centimeter) are chosen larger than in a typical V&F clock. The graphs represent teeth without undercut, and with knife edge rim and flanks.

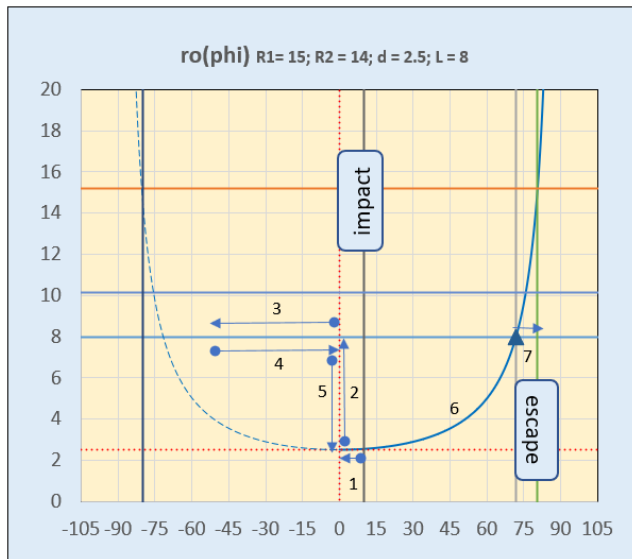


Figure 7

The contact evolution is quite complex, with eight phases in one half oscillation.

1.) After impact, due to the inertia of the foliot the pallet moves against the pressure of the tooth in deceleration, with the outer tooth edge contacting the plane.

2.) At zero arc the contact point jumps to the inner edge of the tooth flank, contacting the pallet rim (vertical line).

3.) The tooth is driven further back by the pallet rim driving the inner tooth flank rim. At a maximum arc the foliot comes to rest.

4.) The direction of motion is reversed under the pressure of the tooth. Now the inner tooth flank rim drives the pallet rim.

5.) At zero arc the contact point jumps to the outer edge of the tooth flank rim contacting the pallet plane.

6.) The pallet plane is driven by the outer tooth edge of the tooth, till it reaches the pallet rim at the vertical gray line.

7.) The tooth rim slides along the pallet rim till its outer edge loses contact at the vertical green line.

8.) After release, the foliot will progress further under its inertia to arcs beyond the contact range, while the opposite tooth has hit the opposite pallet, decelerating the foliot till it comes to rest and reverses direction again.

The main phases are analogous to everyday experiences of friction:

- Tooth in contact with pallet plane: needle scratching along a plane surface.
- Pallet rim in contact with tooth flank: two knife edges scratching along each other.

Figure 8 shows the typical trace of the outer tooth edge at the pallet plane during the long accelerating phase (6). Here the parameters are chosen as in a turret V&F clock: $R1 = 15\text{cm}$; $R2 = 14.5\text{ cm}$; $d = 1\text{cm}$; $L = 2.5\text{ cm}$. In red, the trace at the pallet plane is shown with these parameters.

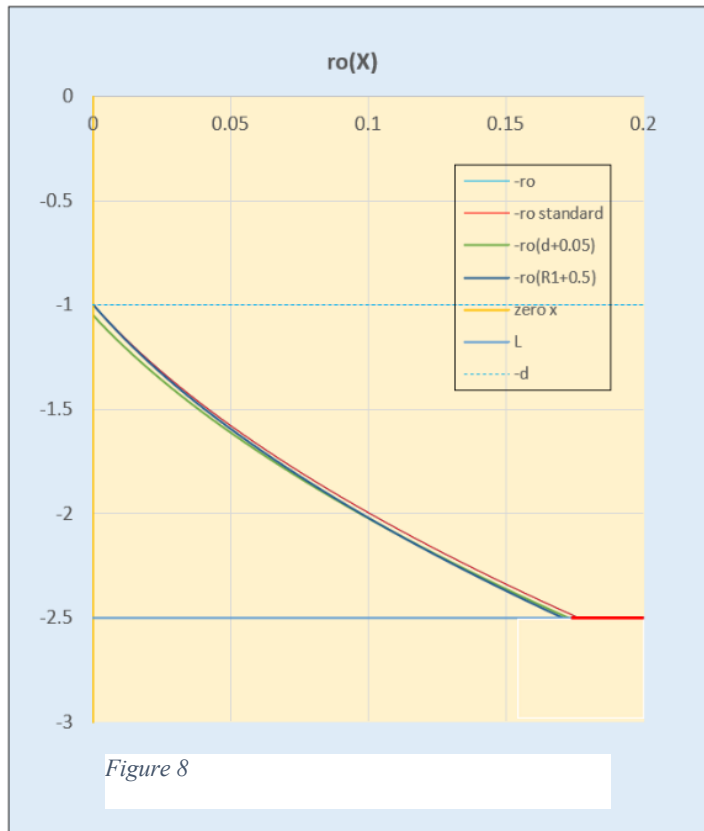


Figure 8

At arc zero the trace starts at distance $-d$ from the verge axis and moves toward the pallet rim $-L$ in a curved line. Then the outer tooth edge escapes, and the tooth rim slides along the pallet rim at constant distance L from the verge axis, till final escape at the pallet inner edge.

To illustrate the influence of tolerances, two additional curves are shown. For the green one, d was increased by 0.05, corresponding to a difference in tooth height of 0.05 cm. For the black one the outer radius of the tooth was increased by 0.5, corresponding to a radial displacement of 0.5 cm. At constant tooth height, the traces start at the same point and then drift apart. For different tooth height, the traces start at different points d , and cross each other.

The issues important for experimental verification are:

1. There exists a distinctive curved trace of point contact at the pallet plane.
2. Tolerances between individual teeth will lead to different parallel or crossing traces.

The derived arguments also hold when the flanks and rim edges of the tooth are not straight but rounded, as by wear. Then the point of contact will wander around the rim and edges during oscillation.

Experimental evidence

Evidence of pointwise contact in the Verge Escapement

The following experimental results were obtained with a newly constructed V&F clock of very low friction bearings. The escape wheel has 43 teeth; The foliot period is 8.37s. One hour corresponds to 430 foliot periods.

High pressure at the contact point should lead to considerable abrasion within a short time. Indeed, with pallets and teeth of steel, one visually observes black smudge within initially clear grease after just a few hours of operation.

Abrasion at the pallet will be higher than at a single tooth, as interaction is n -fold there, with $n = 43$ the number of teeth.

To get reproducible results, runs of several weeks duration were started with new pallets of spring steel, chosen because of its well-defined flat surface, in combination with teeth of mild steel. They were lubricated just once, at start. The edge of the pallet was ground and polished at 45 degrees. Figure 9 shows photos of the pallet surface under different inclinations and illuminations, after 50

days of operation under constant parameters. The clock was run at the arc of close to negligible thermal variation [10] (oscillation within ± 50 degrees), and with an 8s- remontoir for constant drive. Thus, the predominant influence on operation was friction.

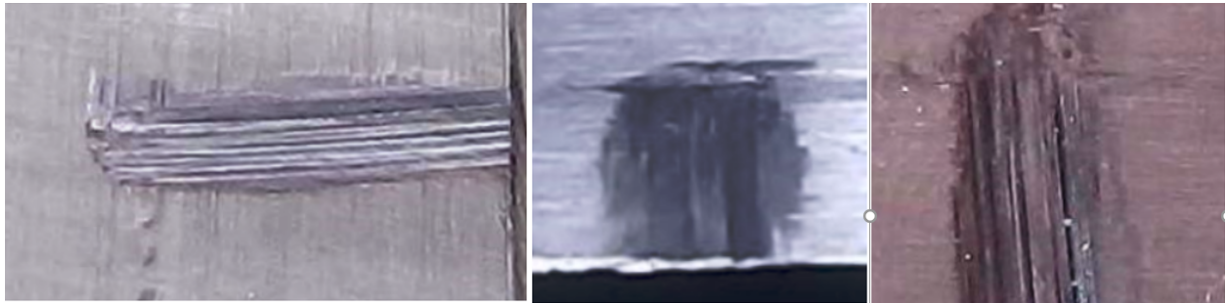


Figure 9

In the photos, the overall curvature of the average contact trace is well visible. One recognizes a slightly varying length of the path, which corresponds to a variation in arc.

The dimensions of the pallets are 20mm x 20mm, those of the scratches 2.0 mm x 8.0 mm.

The deep lateral incisions of the plane are direct indication of a close to pointwise contact. The wear along the pallet rim can be recognized.

The abrasion depth is between 1/100 to 1/10 mm, the amount of removed material larger than $0.001 * 0.2 * 0.5 \text{ cm}^3 = 10^{-4} \text{ cm}^3$. At a density of 7 g/cm^3 the removed material has a mass of $7 * 10^{-4} \text{ g}$, which corresponds to the order of $10^{-4} * 10^{22} = 10^{18}$ atoms. The 5 weeks run duration corresponds to $3.6 * 10^5$ Periods of 8.37s. This results in an abrasion of $10^{18} / 3.6 * 10^5 \approx 3 * 10^{13}$ atoms per period. Considered at the atomic scale, this is an impressively high value, resulting from numerous changing point events along a single trace.

In the photos, the total path at the pallet has a width of about 2 mm, which corresponds to about the thickness of the teeth. Measurement of the tooth tip axis radius gave a maximum variation of about 0.25 millimeter, less than the path width. This seems to contradict the claim of pointwise interaction.

For further study, a short a run of 4 hours was performed, with the verge position lowered to separate the path from the former long-time path. The result is shown in fig 10, under different illuminations.



Figure 10

The left pattern is that of the long run. The right pattern demonstrates the overall path being much thinner in the short run than the tooth width.

The detailed photo reveals that even in the short run there are several very thin grooves. Their distance is in accordance with the variation of the radii of the teeth.

This leads to the following model: with a new plane pallet surface, the first tooth creates a microscopical thin and deep groove by abrasion. Following teeth with close to identical radius R and depth d will deepen and broaden that groove. Teeth with markedly different radius and depth will create slightly displaced and overlapping grooves. At some time, friction has eroded the originally leading edge of teeth and the contact point shifts along the tooth width: the pattern will fill the full tooth width and the interaction point may walk back and forth along it.

As during such a shift other teeth dig into old grooves, the process is accompanied by unpredictable jumps in friction.

An analogy consists in a pointed stick digging across a plowed field along or slightly oblique to the furrows.

To minimize the possibility that the effect is produced by a vertical shift of the verge under influence of moisture or temperature on the suspension filament, the foliot was suspended by a thin strip of *invar* steel. It could have happened that the verge vertical position had changed by some unknown mechanical disturbance. Yet, similar patterns were registered at different new pallets in independent runs (corresponding with figures 9, 10).

It should be noted that the pressure of the teeth on the pallets has a substantial component in the up or down direction of the verge, varying with arc. Together with the elasticity of the suspension, these would assist microscopic vertical shifts at a corroded pallet surface.

Independently of these abrasion effects, a scatter in period could be caused by lateral shifts of the escape wheel axis, affecting d . To limit this, its position was fixed by an axial ball bearing at the end of the shaft, against which the axial component of the torque was pressing. Yet, with the high leverage of the effect some contribution to scatter cannot be excluded.

The experimental result indicates that the average friction is accompanied by a multitude of stochastic changes at the atomic time scale, that will add up to a corresponding stochastic element in the verge period. It also indicates that there are random changes in the mean contact paths, that should show up as longer-term stochastic contributions.

Experimental evidence on stochastic components at the foliot period level

The following experimental result were obtained with a newly constructed V&F clock of typical turret clock dimensions [9].

Foliot period was measured with an optical gate and a digital PC-stopwatch of 1/1000 s resolution. No care was taken tuning the mean period to exactly its nominal period of 8.37s in standard time, as the interesting issue was changes in clock time.

Figure 11 shows foliot period p for 9 revolutions of the crown wheel of 43 teeth. The vertical grid indicates one revolution. Period varies within about ± 0.1 s. One recognizes some periodic patterns per revolution, due to nonuniformities of the teeth. In addition, there is random fluctuation within close limits, contributing about 50% of the total scatter.

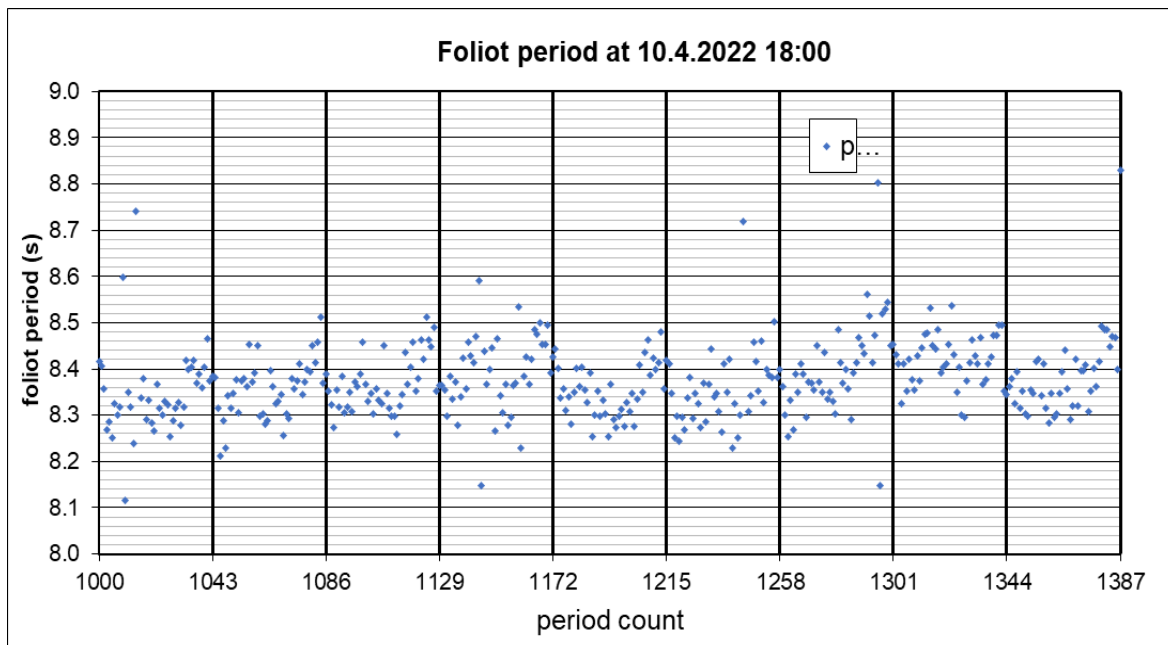


Figure 11

Figure 12 shows fluctuations for the first 1300 revolutions of the escape wheel in the same experiment, including the data of Figure 11. At this larger time scale, wild fluctuations of longer time duration are visible, than cannot be accounted for by any periodicity in the clock.

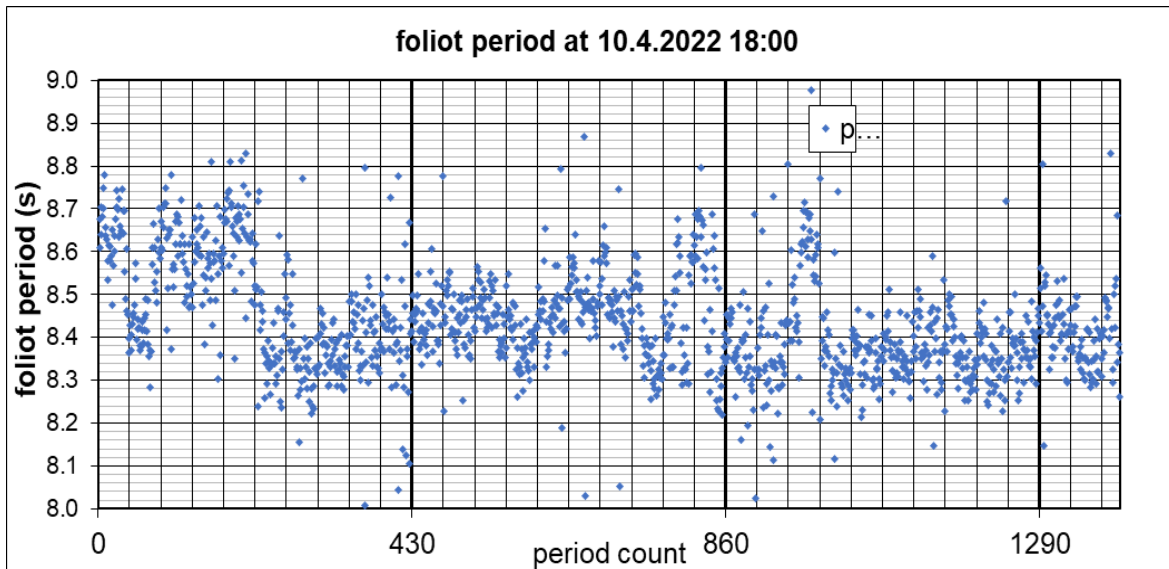


Figure 12

In view of the last paragraph, they are interpreted as random shifts of the active contact zone, while the limited fluctuation in fig 11 shows random fluctuation of friction at momentarily established local friction patterns. It is to be noted, that in the large fluctuations the short-term random part is about the same as in more stable periods.

Figure 13 compacts period (left) and scatter data (right) of 4 different days in a continuous long run, with four of them at enlarged time scale.

- 10.4.2022
- 24.4.2022
- 17.5.2022
- 10.7.2022

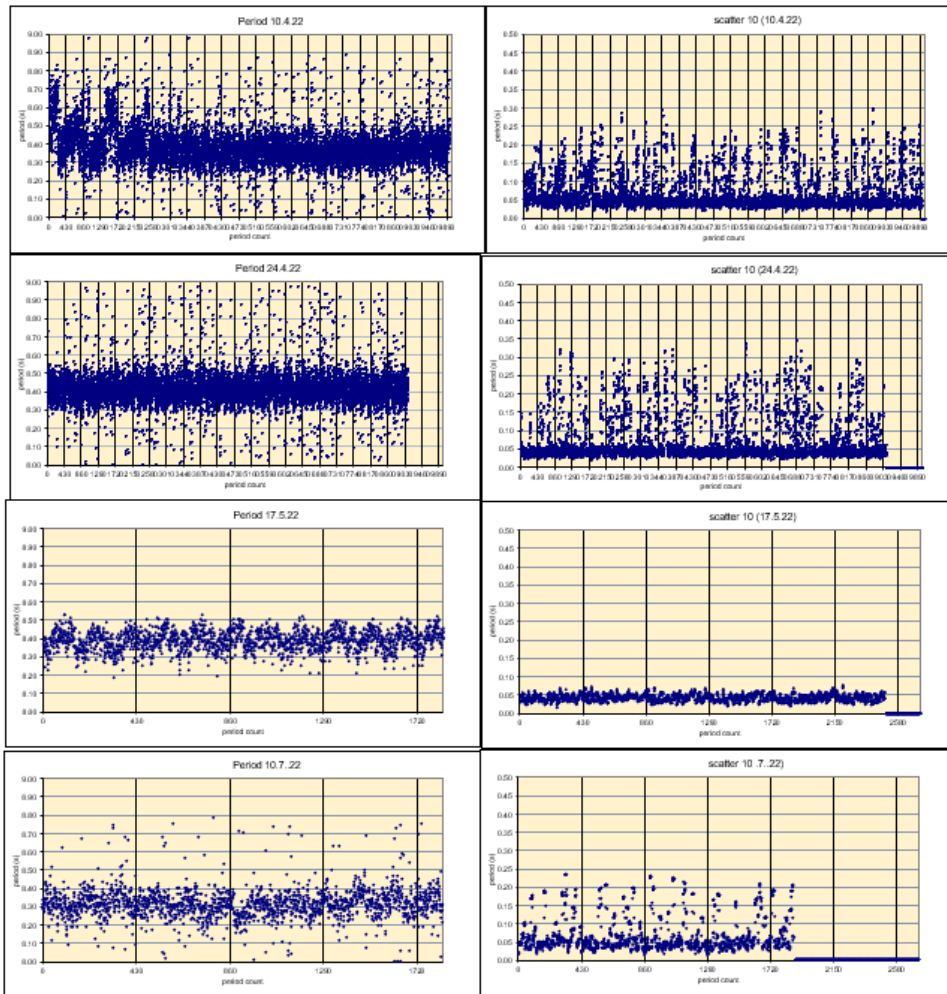


Figure 13

Scatter (*stabwna* in *Excel*) is the variance of data within a given number of samples (here 10 or 50). This measure reduces short time data complexity, while enhancing strong deviations.

The overall picture is that it takes substantial time till large fluctuations become rare, while base scatter reduces early to some average value of 0.04 s. At the short duration of 17.5.22, scatter seems to have settled to a mild equilibrium pattern without large excursions. Yet, the data of 10.7. 22 show that no longer-term equilibrium exists.

Experimental evidence of stochastic influence on clock time

The experiments were extended to observe fluctuation of time at the hour level.

Figure 14 shows the hourly data over the full run of close to 13 weeks (primary vertical grid; the secondary grid indicates days). The upper graph contains the deviation of the hourly periods from the mean, the lower one scatter within 6 hours. There is a 1 ½ week pause caused by travel and a short pause for taking photos of the pallet.

It takes 2 weeks to arrive at relatively stable scatter between 1 to 2 s/h. A few days before and after the longer pause scatter indicates instabilities again.

The experiment ran from 10.4.2022 to 10.7.2022, starting with new pallets. Hourly data were collected by means of a mechanical switch at the barrel wheel and measured in standard time by the digital clock at high resolution. The mechanical uncertainty of the switch was below 0.1s.

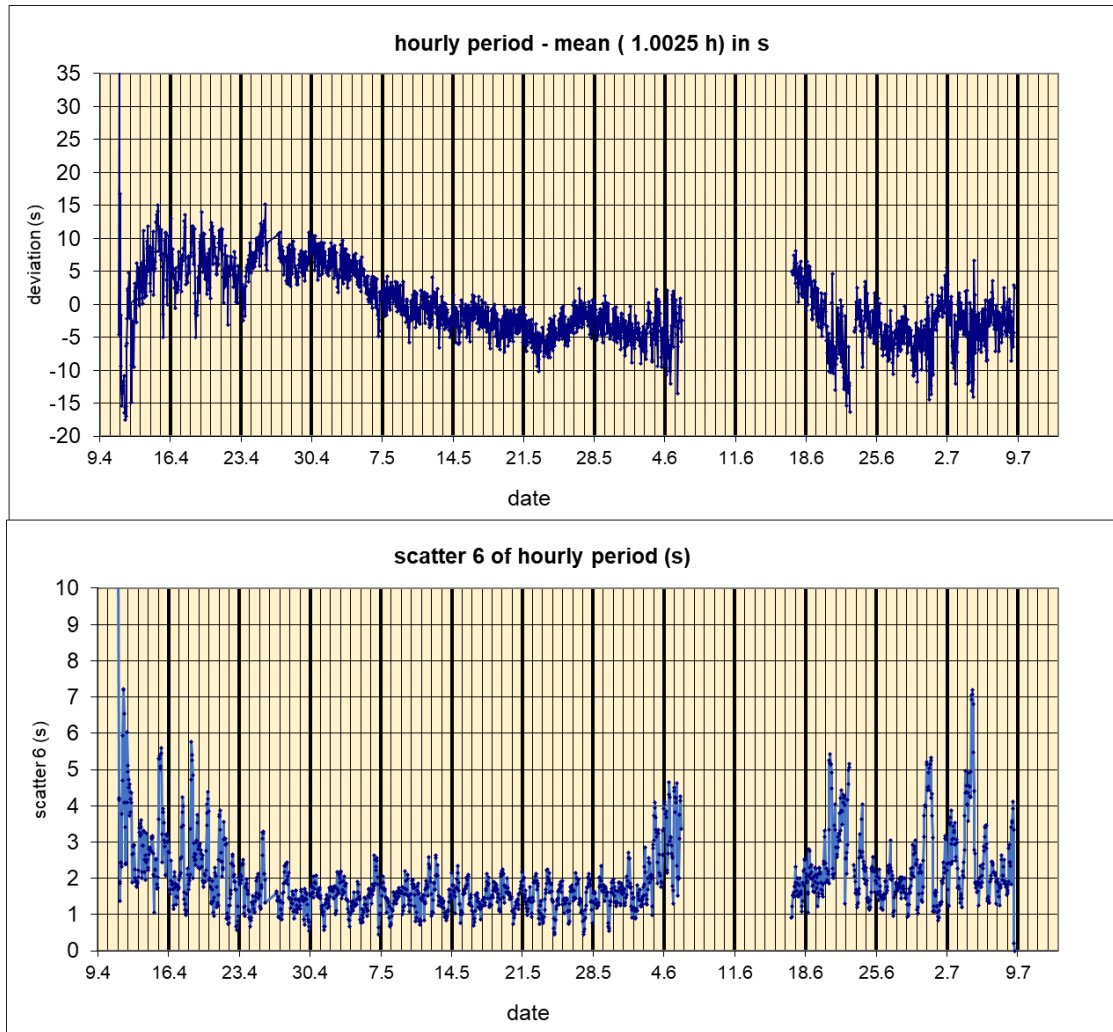


Figure 14

Overall, after a short initial drop, the clock becomes slower for about a week (corresponding to decreasing friction), stabilizes for about two weeks, and then becomes faster for 5 weeks (increasing friction). After the pause, it seems to stabilize again for three weeks, accompanied by increasing strong fluctuations. This overall pattern was reproducible for different runs.

In figure 15 the deviation of total clock time from the average of the first day (*standard clock time*) is shown for 5 independent one week runs with long-used pallets. The pattern looks very much like a random walk. There is one run (red) with fluctuations of just a few seconds per day, that returns to *standard time* after one week. In other runs, daily variations range from part of a minute to 2 minutes, while at the end of the week the deviation from standard time is in the range of one minute to 6 minutes.

In view of the random walk model, the clock could be categorized as having a typical weekly variation of about 2 minutes.

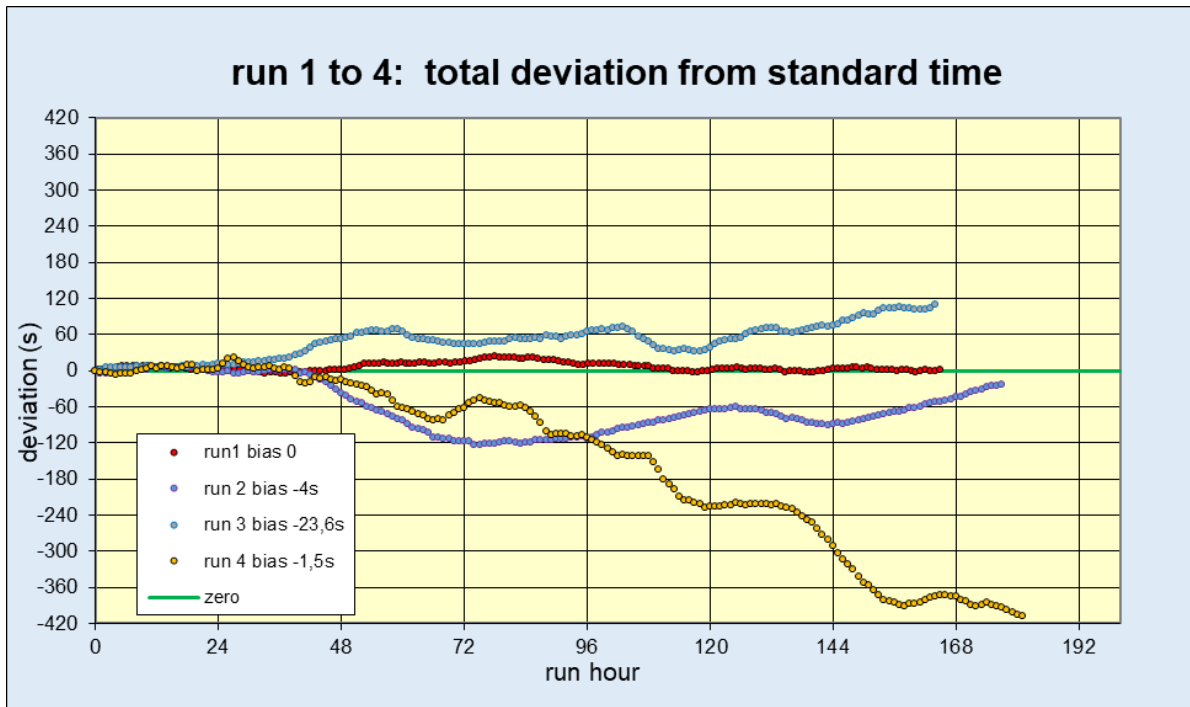


Figure 15

Verge and Pendulum and *Cross Beat* escapement

The verge and pendulum escapement (fig. 16) suffers from the same pointwise friction as the Verge and Foliot one, with strongly reduced total friction energy per period because of the automatic reversal of rotation.

The *Cross Beat* escapement (fig. 17) was an innovation as to friction pressure, while still suffering from the need of high friction energy for reversal of the foliot rotation.

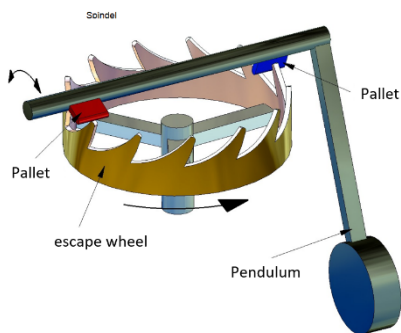


Figure 16

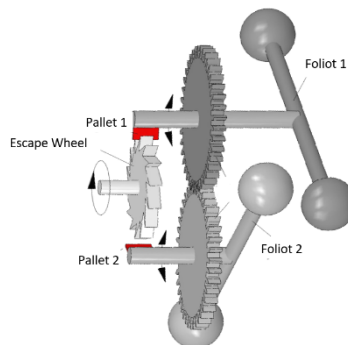


Figure 17

Figures 16 and 17 compare the geometry of the V&P [11] to the one of the *Cross Beat*.

In the *Cross Beat*, there are two foliots, with the corresponding pallets at their respective axis. This allows the foliot axis to be parallel to the one of the escapement wheel.

As consequence, the cylinders around foliot and escapement wheel axis are degenerate and cut in straight lines.

In the *cross-beat* escapement, contact between tooth and pallet is along a line at all arcs. Hence pressure is highly reduced compared to the V&F, at the same friction energy. In comparison to the V&P, it has the advantage of line contact, yet requiring the high friction energy of the V&F for reversal. A knife edge gliding on a parallel surface would be an analogy.

Coupling the two pallets with their separate staffs, which in the V&F and V&P are on a single verge staff, needs an additional, intermediary coupling element - two wheels in the original clock, as shown in the picture. Its gear friction counteracts to some part the advantage of the parallel axis, and Burgi's extreme skill was necessary for the precision of his clock. A number of different coupling alternatives were tried later [1], with no real breakthrough.

The anchor escapement

The anchor escapement (figure 18) with pendulum or spring combines the advantage of parallel escape wheel and pallet axis (low pressure) with the one of automatic reversal of rotation (no reversal energy).

The pallet glides along the tooth tip in a line contact.



Figure 18 [8]

Later improvements optimized the lubrication cushion at the contact line, by proper geometry of the pallets and their separate functions of stopping and accelerating.

A tube gliding (not rolling) on a flat surface would be an everyday analogy.

It should be mentioned here, that as early as 1966 Zheletsov [12] argued that the advantage of the anchor escapement over the verge escapement was positioning the pallet axis *above* the crown wheel axis, without discussing the geometric or physics background. In the same paper the correct differential equation of both oscillators was

described for the first time, in a basic formulation.

With the anchor escapement, an accuracy was achieved where secondary influences became important, and innovative ways for their compensation influenced the further development:

- sensitivity to feedback drive variation, in turret clocks caused for example by the changing rope length, in spring driven clocks by the fading spring power. In both types of clocks, the same principle of a *cone* was used, in turret clocks as a slight taper of the hour wheel barrel diameter (found also in some, not in all V&F relicts), in spring driven clocks by use of a *fusee with chaine*. Its ultimate solution was the introduction of remontoirs, acting on the drive wheel axis or better close to the escape wheel, excluding stochastic friction effects of the clock gear.
- sensitivity to change in arc was minimized in the early verge and pendulum clocks by compensating the pendulum center of gravity curve (*cycloidal cheeks with filament suspension*), in later anchor escapements by restriction to small pendulum arcs (< 4 degrees at close to negligible arc dependence) and by spring suspension.
- sensitivity to temperature change could be minimized in the very sensitive V&F by choice of arcs just beyond the pallet angle [10]; here sensitivity is caused by a complex interaction between different parameters, while the expansion of the foliot is negligible. In the pendulum

clocks thermal expansion of the pendulum staff is important and could be minimized by proper choice of material. In spring balances, compensation by use of bimetal elements was applied.

- sensitivity to changing air pressure and humidity was minimized in pendulum clocks by the use of very heavy pendulums, ultimately by operation in closed tanks a constant pressure and humidity [13].
- Sensitivity to changing feedback from non-constant clock gear was minimized by remontoirs, acting at the hour barrel, or better at the escape wheel, ultimately by complete decoupling over many periods as in the *free pendulum* [14].

The Harrison H4

In view of the above analysis, it appears surprising that Harrison's H 4 with its verge and spring escapement surpassed its geometrically more advanced predecessors so much in accuracy, as it must have suffered from relatively high pressure of the point contact.

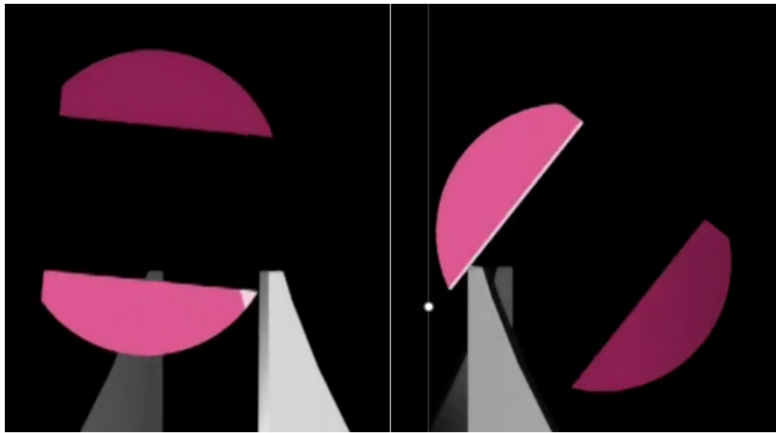


Figure 19 “© www.RedfernAnimation.com”

Figure 19 shows snapshots of the contact between tooth and pallet from the Redfern animations [10].

The realistic perspective along the verge axis demonstrates the point contact, at left when the inner tooth flank drives the pallet rim, at right when the pallet plane is driven by the outer tooth rim edge.

Of course, Harrison had extraordinary watchmaking skills, and he invested many years perfecting parts and bearings. He also invented or introduced the above-mentioned com-

pensating elements, as bimetallic temperature compensation and escape wheel remontoir.

Yet the real clue to the achieved accuracy may lie in the choice of diamond as material of the pallets. As argued above, wear at a pallet will be much more pronounced than at a tooth. With a metal tooth acting on a diamond pallet, there should be practically no wear at the pallet, and the contacting edges of the tooth will be honed to microscopic shape for optimum lubrication in a short time – if not formed intentionally so by the watch maker. This way, stochastic changes in contact point friction are minimized.

Conclusion

The model of contact pressure and abrasion induced by it, causing stochastic changes in escapement friction and hence oscillation period variation, allows to survey the development of mechanical clocks under a uniform physical and geometrical view - from the *Verge and Foliot* clock to the *Verge and Pendulum* or *Verge and Balance* clock, and finally to *Anchor* clocks, and the famous *Harrison H4*.

In the verge escapements contact between pallet and tooth is pointwise, due to perpendicular orientation of their rotation axis. In the anchor escapements contact is along a line, due to parallel orientation of the axis. This results in widely different local friction at equal friction energy per period.

In the pendulum or balance with spring escapements the reversal of rotation is automatic, due to the unidirectionality of the gravitational field or to the symmetry of the spring power. In the foliot escapements reversal is accomplished by friction, which necessitates large friction energies per period.

Geometrical calculation of pointwise contact traces in the verge escapement seem to corroborate well with experimental results of abrasion and period variations obtained with a new, turret-sized Verge and Foliot clock.

On the basis of stochastic period variations, fluctuations against standard time observed in an individual experiment appear as a *random walk* and clock accuracy should be judged on the basis of a minimum number of individual runs.

FINIS

Acknowledgments

These investigations thrived from the cooperation with some friends of ancient clocks, as Malcolm Bell, Merv Hobdon, Robert Cailliau, Donald Saff and Manfred Harig. I am especially thankful to Bob Holmström for his continuous advice and for recently having raised my interest in the wonderful Redfern animations.

I thank *Redfern.animation.com* for the allowance to use snapshots from their simulations in this paper.

Literature

- [1] H. Jendritzki, Hamburg, Schriften der Freunde alter Uhren, Bd. XVII, 1978, S. 117 ff KREUZSCHLAG-VARIANTEN <https://docplayer.org/112146736-Kreuzschlag-varianten.html>
- [2] Christiaan Huygens *Horologium Oscillatorium* 1673
- [3] https://en.wikipedia.org/wiki/John_Harrison
- [4] <https://www.uhrinstinkt.de/magazin/christiaan-huygens-und-die-pendel-uhr/#:~:text=Die%20Ganggenauigkeit%20von%20maximal%20zehn,diese%20Pr%C3%A4zision%20%C3%BCberboten%20werden%20konnte>
- [5] <https://redferanimation.com/the-harrison-timekeepers/#h4>
- [6] von Bertele, H. (1953): “Precision Timekeeping in the Pre-Huygens Era” in *Horological Journal*, Vol. 95, pp. 794–816.
- [7] Kees Grimbergen “Huygens and the Advancement of time measurement” Proceedings of the International Conference “Titan - from discovery to encounter”, 13-17 April 2004, ESTEC, Noordwijk, Netherlands.
- [8] Dieter Roess <https://paw.physik.uni-wuerzburg.de/~roess/NichtSoWichtiges.zip> (5.12.2016) with “Theorie der Waaguhrn des frühen Mittelalters.pdf”; “Waaguhr Neubau Experimente.pdf”; `Java_Simulation_Waaguhr.jar`

- [9] *Dieter Roess* “Theory of the Verge and Foliot Clock of the Early Medieval Age” p. 2 Horological Science Newsletters NAWCC Chapter #161 April 2018
- [10] This topic is treated in an independent paper of the author
- [11] Both graphs [https://de.wikipedia.org/wiki/Hemmung_\(Uhr\)](https://de.wikipedia.org/wiki/Hemmung_(Uhr))
- [12] in A.A. Andronov, A.A.Vitt, S.E. Khaikin *Theory of Oscillators* Dover Publications p. 182 ff.
- [13] Riefler-clocks <https://www.nawcc.org/past-exhibits/precision-clock-gallery/>
- [14] Mannhardt turret clocks <https://clockdoc.org/default.aspx?aid=8179>

Experimental Snippet: Eddy Current Fly

Mike Everman everman@bell-everman.com

The genesis of this experiment came from my interest in creating a mechanical clock that has a truly smooth seconds hand, and therefore a train that does not stop and start as an escapement locks and unlocks. My intent was to rate limit the 5th wheel with eddy current damping, to just a bit faster than needed, and the pendulum gets what it needs bringing that wheel down to rate. I did an experiment about 13 years ago you can easily find on youtube called “eddy current governor”. I wanted to see if I could get a smooth consumption of energy so that my escape wheel would not run away as I somehow sinusoidally impulse the pendulum, which would be a subject for another day. It was quite consistent, but at the time I did not yet have a Microset, and so finer and long-term testing would end up being tedious and coarse. I chalked it up as a Cool Thing, and shelved it until now.

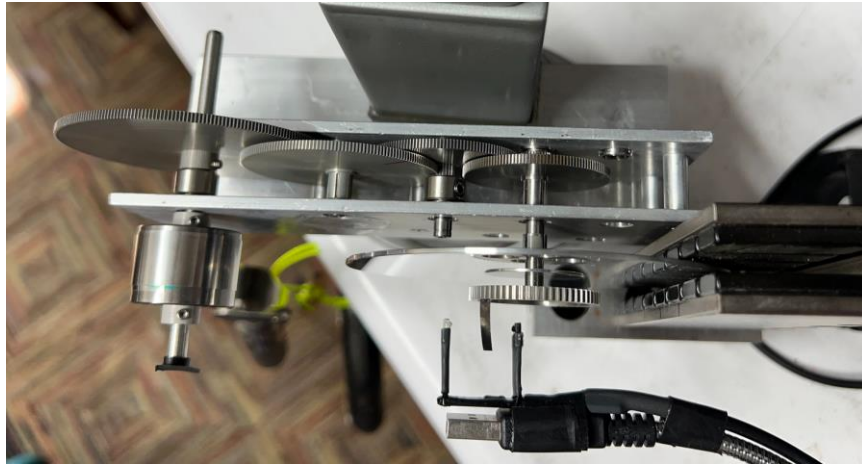
The Eddy Current Effect

Without going too deep into it, eddy currents are created in some non-ferromagnetic metals like aluminum, copper and silver, when passing at right angles through a magnetic field. This creates currents that circulate in the metal, that generate a magnetic field that opposes the metal’s passage through the field. I’ve always been interested in whatever practical use could be made of this effect.

Eddy current dampers were one of the choices back in my spacecraft mechanism days, used to slow the deployment of booms, arrays and antennas to reasonable speeds. The only other practical option was a viscous shear type. The viscous type was mainly used because eddy current types for the larger mechanisms we did would require a step-up geartrain to get the velocity through the field up to a useful level of damping. The added complexity and possible failure points invariably led to using the simpler viscous device for spaceflight. I once made an escapement oscillating a dumbbell that worked quite well, whose sole purpose was eating energy. Again, more parts, so this device quite literally did not get off the ground.

I’ve called this an Eddy Current Fly, because it would fill that role quite well. It has the same character as a typical paddlewheel in air, that is, drag increases with the square of its velocity, and there is zero drag at zero velocity. The rate limit having this exponential relation to velocity makes it far better than a linear proportionality. A fly used as a striking train rate limiter is not required to be incredibly consistent, but if it was, this eddy current approach would be a natural. It would not be affected by changes in the character of the air, and the turbulence of air dampers is just messy.

I recently made a train of gears out of surplus instrument gears and ball bearings, in ratios appropriate for a clock, the first three passes in a configuration of 12:1, 12:1, 5:1, which in this experiment ends with Wheel 4, the 60 second wheel.



On Wheel 4, I added an aluminum hard drive disk substrate taken after fine lapping, and just prior to addition of recordable media, though I do not think that using one with the media would have hurt anything. (Another thing I have many of, sitting around for 30 years, waiting for something like this, that is not a Tesla Turbine!)

The disk is stupendously flat and round, with an OD of 95mm, ID of 25mm, and of 1.5mm thickness. There is a small flag on an extended hub to trip the Microset optical gap sensor once per revolution. The magnet array is an air-core linear motor magnet track segment, with very strong rare earth magnets in alternating pole pairs. A cursory search on the optimization of the eddy current effect suggests that the pole size is to be roughly the same as the disk thickness, which this setup is Decidedly Not. For the higher fidelity attempt, I'll be making a purpose designed set of pole pieces and reducing to one magnet.



The drive method is a 1" mandrel added to Wheel 1, which uses a .003" thick stainless band spirally wrapped a few times, and a roughly 5.5 lb dead weight. The disadvantage of the band-wrap unwinding

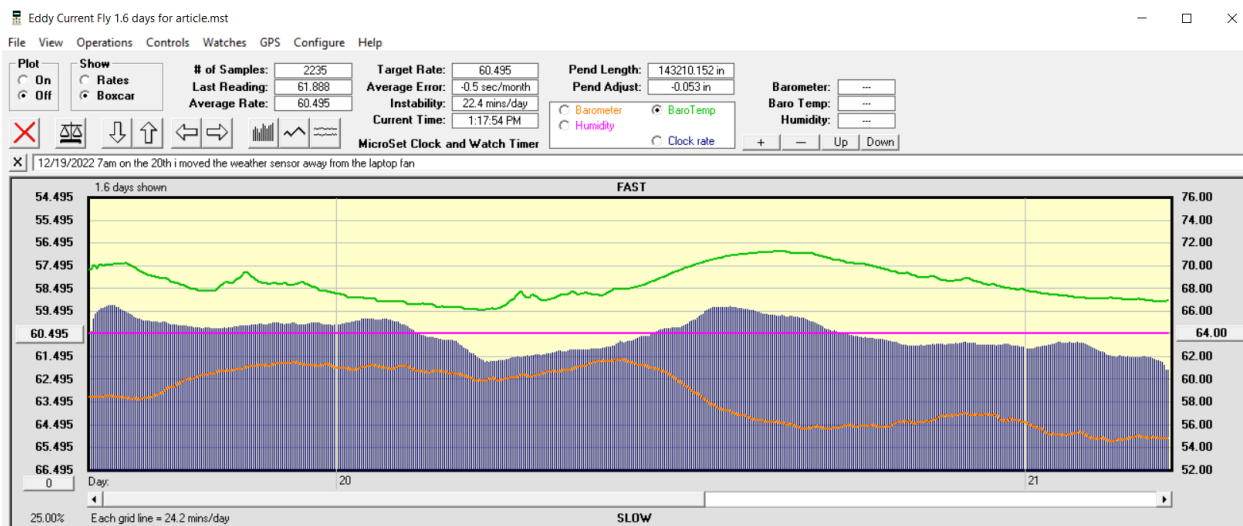
from itself is of course every 12 hours the moment arm of the band reduces by .003”, notching the torque down about 0.6%. This hardware will have to be a bit better to be sure you are seeing that in the plots.

I had thought I would see more variability in the drivetrain; the ball bearings I used were sitting in a box for at least 25 years, so I merely sorted for notional smoothness. The wheels would each have radial run-out, and the center distance for fine teeth like this is generally more critical than the machining I performed, but my goal was simply free rotation, not a perfect mesh. The gears were of dubious provenance as well, some in envelopes with cryptic markings, which may or may not have meant: “do not use this ever”, or loose in a box, which for 96 pitch gear teeth can be death. I had to hand smooth some dings in the teeth, so I had very little expectation of a clean test, but pressed on, and glad I did. To be fair, the un-averaged data is quite noisy, cycle to cycle, but it’s the average that surprised me.

While I am not considering it as a timekeeper in and of itself, it has a quite remarkably stable rate. I’m starting to think that a clock with just this rate limiting device at its heart would be rather good, and worth making.

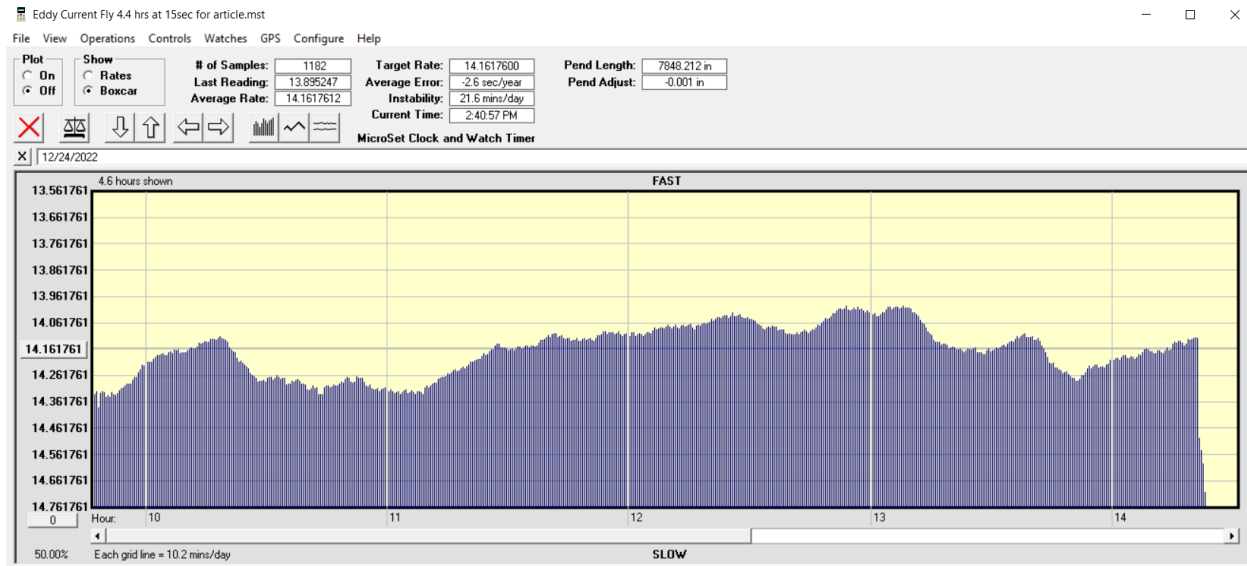
Tests

I did a 1.6 day run with full environmental data. I do not have a fine adjustment for the magnet assembly, so I just attempted to bump it toward 60 seconds (actual average for the test was 60.495s). For this to be in a ± 1.2 second band for the 1.6 day duration is quite unexpected. I’ve applied a 40 count boxcar average to the data.



There may be a temperature correlation, but the magnet assembly is simply resting on the table, so there would be a few too many asterisks applied to any thoughts on that. My first thought was that as the temp goes up, the disk gets bigger and engages with more of the magnetic field, but to verify any correlation here, I would also need understand the reaction time of hardware to air temperature changes, and therefore how much I might mentally shift the temperature graph to the left. It looks like there’s a correlation here (the upper line trace is temperature, the bar graph is rate), but we can’t conclude anything. If the thermal expansion of the disk as temperature rises slows the rate, then a hump in one trace would be coincident with a trough in the other, so the similar shape of the traces is coincidental, and looks to be an unreasonably long reaction time of 7 or 8 hours.

I then did a run where the fly wheel is rotating once per 15 seconds (actual average is 14.16s, no environment data this time), and the average rate is in a band of ± 0.17 s. I'd like to get longer term data for the faster runs, but I'm still limited to a few rotations at Wheel 1.



Preliminary Conclusions

So a factor of approximately four on period improved the error band by a factor of 7 with the same input torque. This meshes nicely with our rather recent acceptance of greater energies in a pendulum, and greater energy per second expended (lower Q or higher entropy) leading to better and faster disturbance rejection. Certainly these gear meshes will smooth out at higher velocity, to a point, blowing through mechanical transients with greater kinetic energy, and there are certainly a host of transients going on in this set of bearings and meshes.

It's difficult to draw parallels with this, as there is no independent resonator at all, so a deeper dive on foliots and other pre-pendulum clocks will be fun. What would the equivalent Q be, anyway, the product of the time the disk coasts down to zero and the period of rotation? The seconds it takes to coast down is certainly not it, being some small fraction of 1. Can I just be happy with this being the king of non-resonant mechanical timekeeping, better than a water clock or hourglass, with no path to precision timekeeping?

When we have a resonator, we only need to replace bearing, windage and escapement losses. This mechanism is entirely about eating the energy we are dumping in, so losses are almost total, with practically no energy stored in the wheel. The data shows it has great promise for consistency of energy conversion. I have resigned myself to electrically wind a clock made with this rate limiter, so I am not for now fighting a stored energy budget.

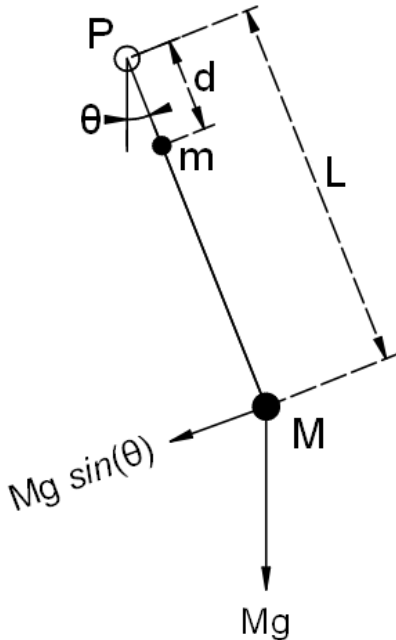
I do think I should make a higher fidelity version, and I may be circling back on the original cable-wrap differential drive, and change the going train for an unloaded counting train. Stay tuned!

The mechanics of a compound pendulum comprising two point masses

by Martin Rice

This investigation was prompted by the desire to understand the physics behind the case of a turret clock whose time keeping is adjusted by adding or removing relatively small auxiliary masses from a platform attached to the shaft of the clock's pendulum. Famously, this is the strategy used at 'Big Ben':

<https://www.youtube.com/watch?v=5qEPDXDVxvw>



The diagram shows the pendulum pivoted at P, with mass m distance d from the pivot, and mass M distance L from the pivot on the same shaft.

The pendulum is shown at angle θ to the vertical.

Mass M experiences a gravitational force Mg downwards, and hence force $Mg \sin(\theta)$ in the direction shown, tending to make M swing in an arc about P, restoring the pendulum to its vertical rest position. Similarly mass m experiences a restoring force $mg \sin(\theta)$ making it also swing in an arc around P.

The moment of inertia of M about P is ML^2 ; the torque on M is $LMg \sin(\theta)$ about P. Similarly, the moment of inertia of m about P is md^2 and the torque is $dmg \sin(\theta)$.

The total moment of inertia, I , is $ML^2 + md^2$. The total torque, τ , is $(LM + dm)g \sin(\theta)$. Provided θ is small we can approximate that $\sin(\theta) = \theta$, provided we measure θ in radians, and thus the restoring torque, $\tau = (LM + dm)g\theta$.

When a body with moment of inertia, I is subject to torque τ it will experience an angular acceleration $\alpha = \frac{\tau}{I}$ and so, writing α as $\frac{d^2\theta}{dt^2}$ and inserting values for τ and I we get

$$\frac{d^2\theta}{dt^2} = -\frac{(LM + dm)g}{ML^2 + md^2}\theta$$

(The minus sign arises because the acceleration is in the opposite direction to that in which θ is measured.)

The corresponding situation for the simple pendulum is $I = ML^2$ and $\tau = LMg\theta$ and

$$\frac{d^2\theta}{dt^2} = -\frac{LMg}{ML^2}\theta = -\frac{g}{L}\theta$$

The familiar formula for T arises: $T = 2\pi \sqrt{\frac{L}{g}}$

By analogy, the formula for T for the two-mass pendulum is:

$$T = 2\pi \sqrt{\frac{ML^2 + md^2}{g(ML + md)}}$$

This gives an insight into the effect that a mass, m , at distance d from the pivot will have on the periodic time of a pendulum with main bob M distance L from the pivot.

The pendulum at St Nicolas church, Newbury, has a design period of 3 seconds. (Horologists would describe this as having a beat of 1.5 seconds.) Using the formula at the bottom of page 1, we can work out that L is about 2.236412m. (This assumes a point mass for the bob. A calculation taking into account the actual shape of the bob is given later.)

An estimate of the mass of the main bob gives a figure of 97.4kg.

(The bob is 'lenticular'. I have taken the shape to be an ellipsoid, and the volume of an ellipsoid is $\frac{4}{3}\pi abc$. $a = b = 0.2\text{m}$ and $c = 0.075\text{m}$. The material of the bob is taken to be iron, with a density of 7874 kg/m^3)

Experiments using 25gm auxiliary masses added approximately 300 mm above the centre of the main bob have been carried out. The corresponding figure for d is thus 1.936412m.

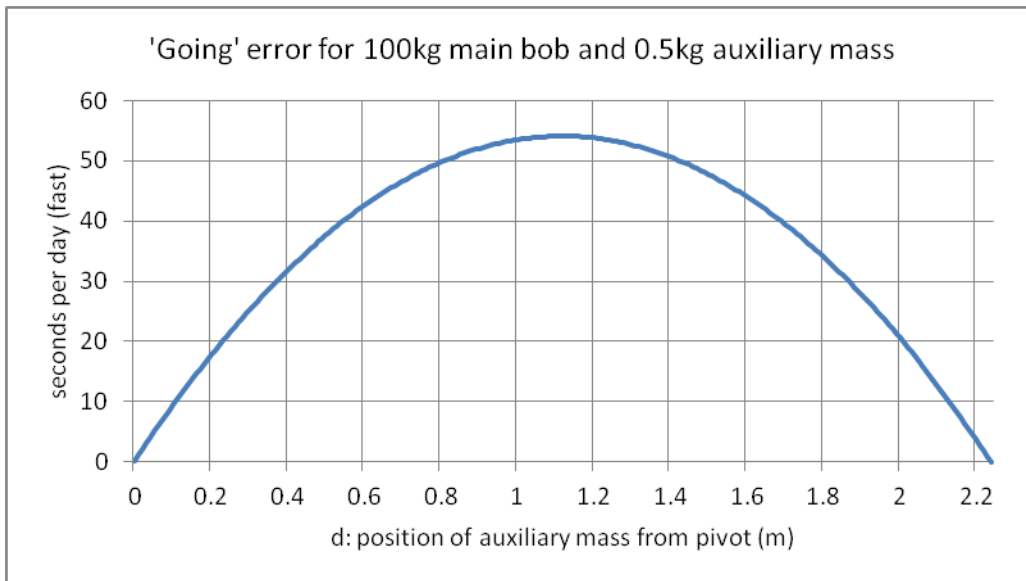
Inserting these data into the formula yields

$$T = 2 \times \pi \times \sqrt{\frac{97.4 \times 2.236412^2 + 0.025 \times 1.936412^2}{9.81(97.4 \times 2.236412 + 0.025 \times 1.936412)}} = 2.999955$$

A little bit faster than 3 seconds! The difference is 45 micro-seconds, but this is over just one period of 3 seconds. Over a day this will amount to $45 \times 10^{-6} \times 60 \times 60 \times \frac{24}{3} = 1.3\text{s}$

The general time-keeping of the clock at St Nic's is subject to apparently random variations on this scale and so it is unclear whether this calculation agrees with experimental evidence, but it would seem to be in the right ball-park. The figure of 0.4 sec/day per old penny given in the Big Ben video would also seem to be plausible, taking into account the pendulum bob of over 200kg, a 4-second period, 9gm for an old penny, and the platform position being the top of the cylindrical pendulum bob.

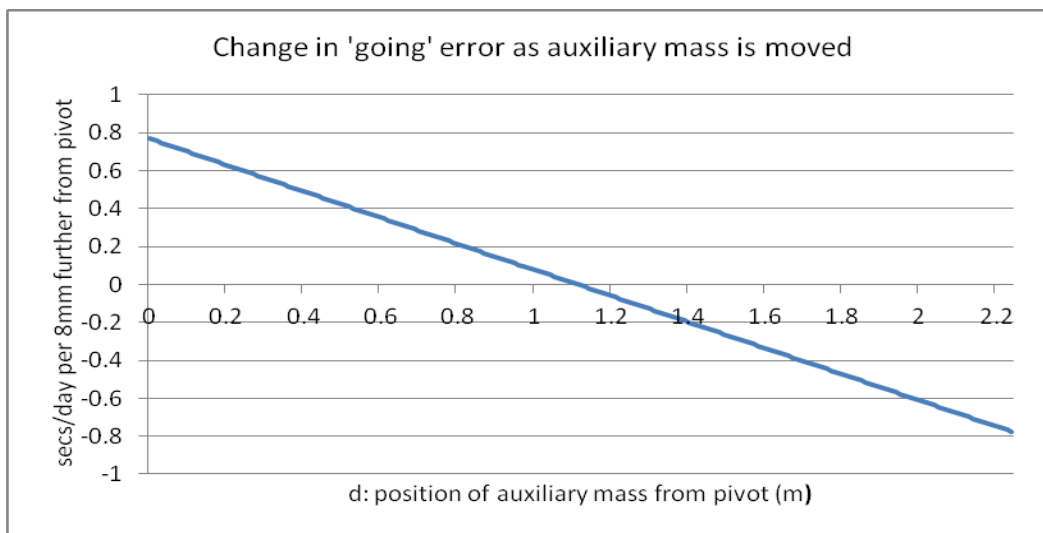
To get a feel for how the position where the auxiliary mass is placed affects the time-keeping I used Excel to repeat the calculation for d varying from 0 to the full 2.236m. The figures for M and m were changed to 100kg and 0.5kg respectively.



The graph shows the error in the going rate in seconds per day. You can see that placing the 0.5kg auxiliary mass half way down the shaft ($d = 1.12\text{m}$) would speed up the pendulum by almost one minute per day. Adding mass at the pivot point itself ($d = 0$) obviously has no effect on the time keeping, nor does adding mass at 2.236m , i.e. increasing the mass of the main bob, as one would expect.

The graph appears to be parabolic. A good matching equation for this data set is $\text{going error} = -43.27d^2 + 96.77d$

Adding and removing auxiliary masses from a platform attached to the pendulum shaft is a good way to 'tweak' the time-keeping, and is easily done by human intervention. In order to provide automatic regulation, however, this is not straightforward. A system employing a small motor to move an auxiliary mass up or down the shaft is quite possible, though, and the question now arises of what is the time-keeping effect of doing this: what is the effect, say, of moving the auxiliary mass from $d = 1.80\text{m}$ to $d = 1.81\text{m}$ (a distance of 10mm)? This amounts to calculating the *slope* of the graph above.

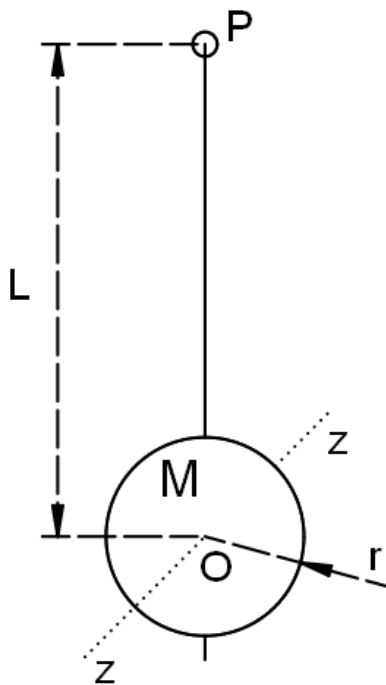


Inspecting the graph at the bottom of P3 shows that the going will change by about -0.5 sec/day for an 8mm movement of the auxiliary mass away from the pivot point. In other words, it will slow down by 0.5 seconds when moving from 1800mm to 1808mm down the shaft.

Interestingly, it would *speed up* by 0.6sec/day if it was moved down from 200mm to 208mm from the pivot. And it wouldn't change at all if moved from 1120mm to 1128mm.

The mechanism I have built to regulate the St Nic's clock comprises a stepper motor driving a length of M5 threaded rod, which has a pitch of 0.8mm/turn. 10 turns of the motor will thus result in an 8mm movement of the auxiliary mass, and about 0.5 sec/day change to the going. The length of the threaded rod allows for a total movement of about 200mm of the auxiliary mass, giving roughly ± 5 sec/day control.

Appendix: even a single mass pendulum is really a compound pendulum.



The diagram shows a pendulum suspended from pivot point P. The bob has mass M, radius r, centre O. It is assumed to be spherical or ellipsoidal (lenticular). The centre of the bob is distance L from the pivot.

The z axis is shown and is perpendicular to the plane in which the pendulum swings.

The moment of inertia of the pendulum about point P is not simply ML^2 but ML^2 plus the moment of inertia of the bob itself about its centre of mass, O, around the z axis.

This additional moment of inertia is $\frac{2}{5}Mr^2$

The total moment of inertia is thus $M\left(L^2 + \frac{2}{5}r^2\right)$

The equation of motion can be written

$$\frac{d^2\theta}{dt^2} = -\frac{MLg}{M\left(L^2 + \frac{2}{5}r^2\right)}\theta$$

and the periodic time is thus $T = 2\pi\sqrt{\frac{5L^2+2r^2}{5Lg}}$

For a 3-second period, and taking r to be 0.2m, this gives $L = 2.229$ m. (Compare $L = 2.236$ m for the simple pendulum.) Since the equation is a quadratic, there are two solutions. The other is $L = 0.007$ m, i.e. 7mm above the centre of the bob.